Kinetics of dimer F_2 type center annealing in MgF$_2$ crystals

V.N. Kuzovkov[a,*], E.A. Kotomin[a,b], A.I. Popov[a]

[a] *Institute of Solid State Physics, Kengaraga 8, Riga LV 1063, Latvia*
[b] *Max Planck Institute for Solid State Research, Heisenbergstr. 1, Stuttgart 70569, Germany*

ARTICLE INFO

ABSTRACT

In this paper, we analyzed experimental annealing kinetics of the primary electronic F centers and dimer F_2 centers observed in MgF$_2$ at higher radiation doses and temperatures. The developed phenomenological theory takes into account the interstitial ion diffusion and recombination with the F_2-centers, as well as mutual sequential transformation with temperature growth of three types of experimentally observed dimer centers: $F_2(1)$, $F_2(2)$, $F_2(3)$ (which differ tentatively by charges $(0, +1, +2)$ with respect to the host crystalline sites). The results of the electron, neutron and ion irradiation are compared. As the result, the relative initial concentrations of three types of F_2 electronic defects before annealing are obtained, along with energy barriers between their ground states as well as the relaxation energies.

1. Introduction

Primary radiation defects in ionic solids consist of Frenkel defects—pairs of anion vacancies with trapped electrons (F-type centers) and interstitial ions [1–4]. Upon temperature increase after irradiation, the electronic F-type centers are annealed due to recombination with much more mobile interstitials [1,5–9] or become mobile themselves, thus forming more complex electronic centers (dimer F_2-type, trimer F_3-type etc) or even, under certain conditions, creating metallic colloidal particles [10–14]. F_2, F_3 centers consist of 2 or 3 nearest vacancies with trapped electrons [2,11]. The appropriate analysis of the recombination (annealing) kinetics allows us to obtain important information on the interstitial migration [9]. Relevant theoretical models have been developed and described in detail in Refs. [9,15–17]. Note the complex F_2-type, trimer F_3-type electron centers as well as metallic colloids can also be formed at high radiation doses even at temperatures where the F-centers are immobile [18–20]. (This is the case in the present paper.) All the above mentioned processes strongly depend on the type of material, the structure of the crystal lattice, and the efficiency of the corresponding defect formation process [21–23]. Detailed understanding of the radiation damage mechanisms and kinetics is important for improving materials radiation properties.

The situation is more or less well understood in simple NaCl-type structures, of which the alkali-halide crystals and simple oxides (MgO) are representatives [21–30], however in the case of more complex structures, such as fluorides, spinels and rutiles the current level of understanding is still far from the completed [23,30–33]. In many ways, this is due to the lack of sufficient experimental data, which, in turn, is related to a low efficiency of defect formation and a sufficiently high thermal stability of the radiation defects.

Among the materials with a complex crystalline structure, MgF$_2$ crystals, in particular, were extensively investigated due to their excellent electronic and optical properties and use as lenses, optical window, in laser active elements etc [34]. MgF$_2$ has a tetragonal (rutile) structure with the unit cell consisting of $2\,Mg^{2+}$ and $4\,F^-$ ions. This structure allows defect configurations different from those observed in the NaCl–type alkali halides and simple oxides or the fluorite-structured alkaline earth halides (CaF$_2$, SrF$_2$ and BaF$_2$) [35–37].

MgF$_2$ has attracted the attention of a number of researchers in the context of irradiation-induced defects and radiation damage mechanisms. Various types of radiation defects were observed and studied in MgF$_2$ under irradiation with various types of ionizing and particle radiation, including VUV, γ- and X-ray radiation, fast electron, neutron, high energy protons and GeV heavy ions [38–45]. Just as in the case of alkali halides and MgO and Al$_2$O$_3$, defects in MgF$_2$ can also be created without irradiation, namely, by additive coloration (TCR) [39]. Such F and F-aggregate centers were produced in high concentration, when crystal is heated to a high temperature and under high Mg vapour pressure.

As known from experiments with ^{60}Co, γ-rays, X-rays, electrons, neutrons and more recently also with low-energy ions [36,38–46], the most dominant band with maximum optical absorption at 255–260 nm is due to the single F-centers.

The other absorption bands at 320 and 370 nm were ascribed to F_2-centers (two electrons localized at two neighbouring anion vacancies) with different orientations in the tetragonal lattice, called F$_2$(1) with

* Corresponding author.
 E-mail address: kuzovkov@latnet.lv (V.N. Kuzovkov).

D_{2h} and $F_2(2)$ with C_{2h} symmetry [46]. The optical absorption band at 430 nm is attributed to $F_2(3)$ – another F_2-centers of unknown symmetry, appearing only after irradiation at high ion fluencies [46]. The exact position of the band is difficult to determine, since it lies on the tail of the more pronounced $F_2(2)$ component. Note that charge state of these F_2 centers is unknown.

Note also, that in the studies [47,48] the appropriate positions of the bands are given at 255, 320, 370 and 400 nm at 300 K in heavy ion irradiated MgF_2 [47], while Nakagawa et al. [49] instead of previous assignment gave rather different interpretation. Four different types of the *F-F* vacancy bonds in MgF_2 could be possibly associated with the observed F_2 absorption: the 300 nm band to the $F_2(D_{2h})$, the 325 nm band to the $F_2(C_1)$, the 355 nm band to the $F_2(C_{2v})$, and the 400 nm band to the $F_2(C_{2h})$ centers [49], while 430 nm band is hardly related to the F_2 centers. Complicated character of the optical absorption spectra in the region of the F_2 absorption has been also emphasized in Refs. [42,43]. In particular, both Davidson et al. [42], Amolo et al. [43], and earlier Nakagawa et al. [49] have suggested the emergence of the Mg–colloid absorption band produced at 290–300 nm. In this paper, we follow F_2 band interpretation suggested in Ref. [46].

Inlike the electronic *F* centers, their complementary Frenkel partners – interstitial fluorite ions in MgF_2 are practically unstudied, neither experimentally nor theoretically. It was suggested [35] that stable and low mobile interstitial molecules F_2 are formed which decay at relatively high temperatures. This is in agreement with two hole centers observed experimentally by Ueda [50], one of them (produced in MgF_2 crystals irradiated with γ-rays and neutrons at low temperature and designated as H_N) was assigned to an interstitial fluorine *F* atom which forms an asymmetric ($F^{-0.4}$–$F^{-0.6}$) molecular ion with a lattice F ion, decays at 560 K. Probably, thermal decay of such or similar centers is responsible for the main annealing stage of the *F* centers in MgF_2. The *F* center annealing upon sample heating was studied more than once (depending on radiation dose and type of radiation) in the temperature range between 500 K and 800 K.

The general methodology for describing and analyzing a dynamic many-body system in its complexity taking into account its physical (interactions between components: particles, molecules, clusters etc) and chemical (reactions) properties was introduced and discussed by us in Refs. [51–59]. In particular, recently we developed phenomenological theory describing the diffusion-controlled kinetics of radiation defect annealing in ionic solids [9,15] and demonstrated how its fitting to the experimental curves allows one to extract two control parameters: the migration energy of the interstitial ions E_a and the pre-exponent $X = N_0 R D_0 / \beta$, where N_0 is initial defect concentration, R recombination radius, D_0 diffusion pre-exponent, and β heating rate. Assuming standard parameters $N_0 = 10^{17}\,cm^{-3}$, $R = 10\,Å$, $D_0 = 10^{-3}\,cm^2\,s^{-1}$, $\beta = 10\,K/min$, one gets the estimate $X = 10^8\,K^{-1}$ for a normal diffusion. In this paper, we analyzed available experimental kinetics of the single *F*- and dimer F_2 type center annealing in MgF_2 in a wide temperature range (300–800 K).

2. Results

2.1. The F centers

The *F* centers in MgF_2 show a distinctive optical absorption at 255 nm [45,46]. The results of theoretical analysis of the *F* center annealing in MgF_2 irradiated by electrons, neutrons and heavy ions are presented in Fig. 1 and Table 1. The first conclusion is a big variation of the E_a, and X parameters depending on the irradiation dose. In particular, increase of the electron irradiation fluence (dose) by a factor of 20 leads to a dramatic reduction of E_a, from 1.6 eV (normal diffusion, $X = 10^8\,K^{-1}$) down to 0.35 eV (anomalous diffusion, $X = 3.5 \cdot 10^0\,K^{-1}$). Similar effects take place also under neutron irradiation. Decrease of the diffusion energies is accompanied with the decrease by orders of magnitude of the pre-exponential factors. This is not result of bad fitting
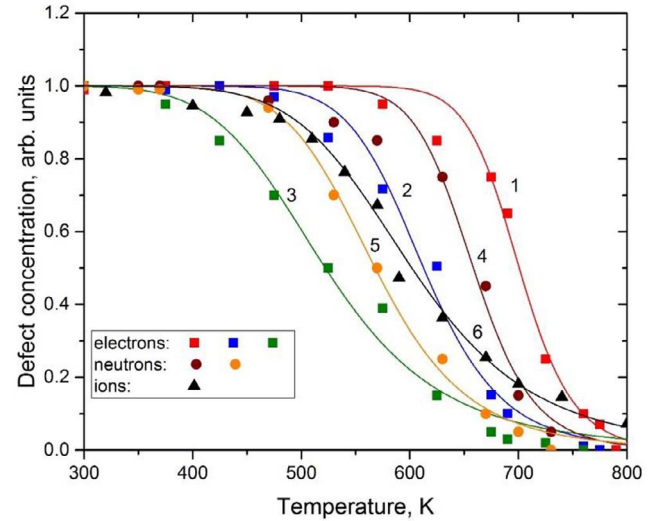

Fig. 1. The kinetics of the *F* center annealing after exposure to three types of radiation (see Table 1 for details). The electron irradiation under 3 different doses – curves 1–3 [45], neutrons under two fluences – curves 4, 5 [45] and heavy U ion irradiation – curve 6 [46].

Table 1
The explanation of curves 1–6 in Fig. 1 and the obtained migration energy of interstitial ions E_a and pre-exponential factor X under different types of radiation and different doses.

Nr.	Legend	E_a (eV)	X (K^{-1})	Reference
1	EPR, electron irradiation dose $1 \cdot 10^{16}$ electrons/cm^2	1.60	$1.0 \cdot 10^8$	[45]
2	EPR, electron irradiation dose $1 \cdot 10^{17}$ electrons/cm^2	0.80	$8.4 \cdot 10^3$	[45]
3	EPR, electron irradiation dose $2 \cdot 10^{17}$ electrons/cm^2	0.35	$3.5 \cdot 10^0$	[45]
4	EPR, neutron irradiation, 15 min	1.24	$9.8 \cdot 10^6$	[45]
5	EPR, neutron irradiation, 10 h	0.56	$1.8 \cdot 10^2$	[45]
6	Optical absorption, U ions (11.1 MeV/u) of fluence $6 \cdot 10^{11}$ cm^{-2}	0.46	$9.6 \cdot 10^0$	[46]

– theoretical curves are very smooth and close to the experimental points at all conditions. We believe that the observed diffusion parameter dependence on the radiation dose and correlation between E_a and X are related to the increased material disordering under increasing irradiation dose which will be discussed in oncoming paper [60]. Thus, the largest migration energy of 1.6 eV is attributed to the interstitial (hole center) migration energy in almost perfect crystal. Very likely, this energy corresponds to the above mentioned interstitial delocalization from traps (impurities) or interstitial F_2 molecule dissociation [35], and real migration energy of a free interstitials is considerably smaller.

2.2. Dimer centers

The dimer F_2 centers (electrons trapped by two nearest vacancies) were observed under heavy ion irradiation and characterized tentatively by the absorption bands at 320 nm – $F_2(1)$, 370 nm – $F_2(2)$ and 430 nm – $F_2(3)$ [46]. Authors assume that "under annealing the $F_2(1)$-centers are probably converted into $F_2(2)$- or $F_2(3)$-centers before finally recombining with hole centers".

The normalized annealing kinetics of the *F*- and three F_2-centers are plotted in Fig. 2. As one can see, concentration of the single *F* centers monotonous decreases (see also Fig. 1) whereas three dimer centers show very different behavior: similar but faster monotonous decay for $F_2(1)$, a sharp $F_2(2)$ peak in the temperature range of the $F_2(1)$ decay, and $F_2(3)$ peak at higher temperatures where $F_2(2)$ centers decay. Note that the F centers are immobile in the temperature range considered
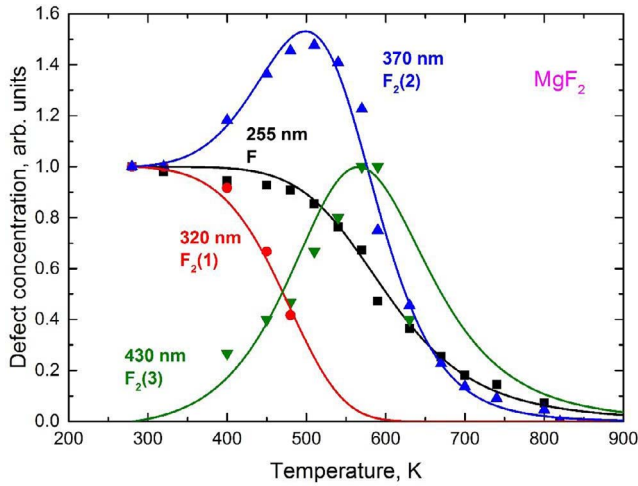
Fig. 2. Experimental points from [46] and their theoretical analysis (full lines). Initial concentrations of the $F_2(1)$ and $F_2(2)$ are taken as unity, whereas for weak $F_2(3)$ band the concentration in the peak maximum was taken for unity.

Fig. 3. The calculated temperature dependence of dimer center populations.

here and thus F_2 centers were created during irradiation rather formed due to the F center diffusion and aggregation.

This supports idea of mutual transformation of three types of dimer centers. The fact that the *F* center decay is not affected by the mentioned peculiarities in the F_2 kinetics indicates at negligible concentration of dimer centers compared to that of the *F* centers. This allows us to treat kinetics of the *F* and F_2 centers independently which greatly simplifies the problem. In particular, while considering the kinetics of dimer centers, the concentration of hole centers could be taken from solution for the kinetics for single centers.

The annealing kinetics of dimer centers is a combination of the two independent processes: recombination of immobile electron centers with mobile interstitials (hole centers) and mutual transformation of three types of F_2-type centers: $F_2(1) \rightarrow F_2(2)$, $F_2(2) \rightarrow F_2(3)$. Let us introduce the dimensionless defect concentrations: $C_F(t) = n(t)/n(0)$. It could be shown that the decay of the total dimer center concentration is related to that of the *F* centers: $C_F(t)^\kappa$, where $\kappa = R_2/R$, R and R_2 are recombination radii for interstitials with single and dimer centers. Three dimers could be characterized by probabilities $W_i(t)$, i = 1,2,3, with the normalization $W_1(t) + W_2(t) + W_3(t) = 1$ and initial condition $W_i(0) = w_i$. The dimer concentrations are defined as products $W_i(t)C(t)^\kappa$. These concentrations are additionally rescaled in Fig. 2, in order to make small peaks more pronounced.

The probabilities to find centers are defined by the following set of kinetic equations:

$$\frac{dW_1(t)}{dt} = -p_1 W_1(t), \tag{1}$$

$$\frac{dW_2(t)}{dt} = p_1 W_1(t) - p_2 W_2(t), \tag{2}$$

$$\frac{dW_3(t)}{dt} = p_2 W_2(t). \tag{3}$$

These equations describe dimer center mutual transformations $F_2(1) \rightarrow F_2(2)$, with the rate $p_1 = p_1^0 \exp(-E_b/k_B T)$, and then $F_2(2) \rightarrow F_2(3)$ (with the rate $p_2 = p_2^0 \exp(-E_c/k_B T)$). The equation set could be numerically solved, provided the constant heating rate $\beta(t) = \beta = const$. By means of the least square method, one can get the main kinetic parameters – activation energies E_b and E_c, two pre-exponents $P_1 = p_1^0/\beta$ and $P_2 = p_2^0/\beta$, recombination parameter κ and initial defect populations w_i. Our analysis shown that $w_3 = 0$, so that $w_1 = 1-w_2$.

The results are shown in Fig. 2 in full curves. As one can see, a simple model describes very well a whole set of experimental data.
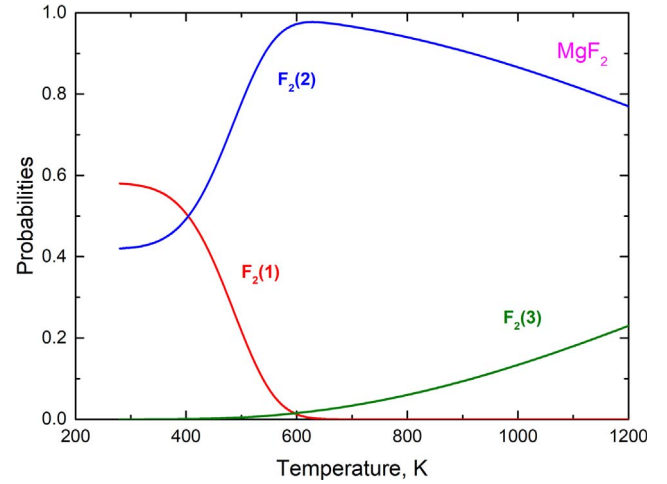
Three calculated activation energies are similar, the interstitial migration energy $E_a = 0.46$ eV (Table 1), and two dimer transformation energies $E_b = 0.27$ eV and $E_c = 0.15$ eV, two of three related pre-exponents are also close, third one is very small: $X = 9.6 \cdot 10^0$ K^{-1}, $P_1 = 8.4 \cdot 10^0$ K^{-1} and $P_2 = 3.0 \cdot 10^{-3}$ K^{-1}. The parameter $\kappa = 1.68$ is close to the ratio of geometric cross sections of a single and double vacancy. Lastly, the initial dimer populations of $F_2(1)$ and $F_2(2)$ are close, $w_1 = 0.58$ и $w_2 = 0.42$ whereas third one, as mentioned above, is negligible, $w_3 = 0$. Note that the obtained activation energy of the interstitial migration $E_a = 0.46$ eV under ion irradiation is much smaller of that for the electron irradiation (Table 1). It could be shown also that there is no transformation $F_2(1) \rightarrow F_2(3)$ whereas successive transformations $F_2(1) \rightarrow F_2(2)$, $F_2(2) \rightarrow F_2(3)$ are irreversible.

Additional information is presented in Fig. 3. The $F_2(1)$ after transforming into $F_2(2)$ practically disappears already at 600 K, whereas $F_2(3)$ is still very small (a few per cent). This is a reason why $F_2(3)$ band is hardly observable experimentally below 600 K [46]. This band starts to grow only above 600 K, but here both $F_2(2)$ and $F_2(3)$ rapidly disappear due to recombination with highly mobile interstitials and thus their concentrations are very low.

It is logical, to assume that three F_2-type centers correspond to three possible *dimer charges*: F_2, F_2^+ and F_2^{2+} which explains also observation of three dimer centers, not two or four. The sequence of dimer center transformations could correspond to their thermal ionization with release each time one electron, $F_2 \rightarrow F_2^+ + e$ and $F_2^+ \rightarrow F_2^{2+} + e$, respectively. Indeed, thermal ionization of point defects is well known process in color center physics [2]. The idea of three different states is also confirmed by similar observation of the dimer centers in Al_2O_3 [61–63] and does not contradict also assumption [46] about different local symmetry of dimer centers.

3. Conclusions

Phenomenological theory of the annealing kinetics of single *F*- and dimer F_2-electron centers in irradiated ionic solids was developed and applied to MgF_2 crystals. Theoretical analysis of the available experimental kinetics for the *F* centers under electron, neutron and heavy U ion irradiations shows similar trend: the interstitial migration energy strongly decreases with the radiation fluence which will be discussed in oncoming paper [60].

Analysis of the kinetics of the mutual transformation of three types of dimer F_2-type centers observed under heavy ion irradiation [46] allows us to extract all kinetic parameters and suggest idea that these centers differ by the charge states (neutral, single- and double-charged defects with respect to the perfect crystal). This hypothesis is supported by our similar results for three types of dimer centers in Al_2O_3 [61–63]

to be discussed elsewhere. In order to understand physical meaning of these kinetic parameters, calculations of the electronic structure and relative stability of dimer centers are necessary [61]. This could permit to discriminate between thermal ionization (electronic process) and spatial reorientation (ionic process) between different dimer configurations.

Acknowledgments

References

[1] Ch.B. Lushchik, I.K. Vitol, A. Elango, Sov. Phys. Usp. 20 (1977) 489.
[2] A.M. Stoneham, Theory of Defects in Solids, Oxford, 1975.
[3] R.T. Williams, Rad. Eff. Def. Solids 109 (1989) 175.
[4] E. Kotomin, A. Popov, M. Hirai, J. Phys. Soc. Jpn. 63 (1994) 2602.
[5] E.A. Kotomin, A.I. Popov, R.I. Eglitis, J. Phys.: Condens. Matter 4 (1992) 901.
[6] R.I. Eglitis, A.I. Popov, E.A. Kotomin, Phys. Status Solidi B 190 (1995) 353.
[7] M. Kirm, A. Lushchik, Ch. Lushchik, I. Martinson, V. Nagirnyi, E. Vasil'chenko, J. Phys.: Condens. Matter 10 (1998) 3509.
[8] A.Ch. Lushchik, A.G. Frorip, Phys. Status Solidi B 161 (1990) 525.
[9] V.N. Kuzovkov, A.I. Popov, E.A. Kotomin, A.M. Moskina, E. Vasil'chenko, A. Lushchik, Low Temp. Phys. 42 (2016) 748.
[10] E.A. Kotomin, V.N. Kuzovkov, A.I. Popov, Radiat. Eff. Defects Solids 155 (2001) 113.
[11] E.A. Kotomin, A.I. Popov, in: E. Kotomin, K. Sikafus, (Eds.), Radiation Effects in Solids, NATO Science Series II-Mathematics Physics and Chemistry, 235 (2007) 153–192.
[12] A.E. Hughes, S.C. Jain, Adv. Phys. 28 (1979) 717.
[13] M.A. Monge, A.I. Popov, C. Ballesteros, R. González, Y. Chen, E.A. Kotomin, Phys. Rev. B 62 (2000) 9299.
[14] A.I. Popov, M.A. Monge, R. González, Y. Chen, E.A. Kotomin, Solid State Commun. 118 (2001) 163.
[15] E.A. Kotomin, V.N. Kuzovkov, A.I. Popov, R. Vila, Nucl. Instr. Meth. B 374 (2016) 107.
[16] V.N. Kuzovkov, A.I. Popov, E.A. Kotomin, M.A. Monge, R. Gonzalez, Y. Chen, Phys. Rev. B 64 (2001) 064102.
[17] E.A. Kotomin, V.N. Kuzovkov, A.I. Popov, M.A. Monge, R. Gonzalez, Y. Chen, Nucl. Instr. Meth. B 191 (2002) 208.
[18] N. Bouchaala, E.A. Kotomin, V.N. Kuzovkov, M. Reichling, Solid State Commun. 108 (1998) 629.
[19] M. Huisinga, N. Bouchaala, R. Bennewitz, E.A. Kotomin, M. Reichling, V.N. Kuzovkov, W. von Niessen, Nucl. Instr. Meth. B 141 (1998) 79.
[20] D. Ochs, M. Brause, W. Maus-Friedrichs, V. Kempter, J. Electr. Spectrosc. Relat. Phenomena 88–91 (1998) 725.
[21] A.I. Popov, E.A. Kotomin, J. Maier, Nucl. Instr. Meth. B 268 (2010) 3084.
[22] S.J. Zinkle, Nucl. Instr. Meth. B 286 (2012) 4.
[23] A. Lushchik, Ch. Lushchik, A.I. Popov, K. Schwartz, E. Shablonin, E. Vasil'chenko, Nucl. Instr. Meth. B 374 (2016) 90.
[24] R.S. Averback, P. Ehrhart, A.I. Popov, A. von Sambeek, Radiat. Eff. Defects Solids 136 (1995) 169.
[25] A. Lushchik, Ch. Lushchik, M. Kirm, V. Nagirnyi, F. Savikhin, E. Vasil'chenko, Nucl. Instr. Meth. B 250 (2006) 330.
[26] M.A. Monge, R. Gonzalez, J.E. Santiuste, R. Pareja, Y. Chen, E.A. Kotomin, A.I. Popov, Phys. Rev. B 60 (1999) 3787.
[27] A. Lushchik, C. Lushchik, K. Schwartz, F. Savikhin, E. Shablonin, A. Shugai, E. Vasil'chenko, Nucl. Instr. Meth. B 277 (2012) 40.
[28] M.A. Monge, R. Gonzalez, J.E. Santiuste, R. Pareja, Y. Chen, E.A. Kotomin, A.I. Popov, Nucl. Instr. Meth. B 166 (2000) 220.
[29] A.I. Popov, E.A. Kotomin, M.M. Kuklja, Phys. Status Solidi B 195 (1996) 61.
[30] E.A. Kotomin, A.I. Popov, A. Stashans, J. Phys.: Condens. Matter 6 (1994) L569.
[31] N. Mironova-Ulmane, V. Skvortsova, A. Pavlenko, E. Feldbach, A. Lushchik, Ch. Lushchik, V. Churmanov, D. Ivanov, V. Ivanov, E. Aleksanyan, Radiat. Meas. 90 (2016) 122.
[32] Yu.F. Zhukovskii, A. Platonenko, S. Piskunov, E.A. Kotomin, Nucl. Instr. Meth. B 374 (2016) 29.
[33] M. Kirm, A. Lushchik, Ch. Lushchik, A.I. Nepomnyashikh, F. Savikhin, Radiat. Meas. 33 (2001) 515.
[34] W. Hayes, A.M. Stoneham, Crystals with Fluorite Structure, Clarendon Press, Oxford, 1974.
[35] F.U. Abuova, E.A. Kotomin, V.M. Lisitsyn, A.T. Akilbekov, S. Piskunov, Nucl. Instr. Meth. B 326 (2014) 314.
[36] V.M. Lisitsyn, L.A. Lisitsyna, A.I. Popov, E.A. Kotomin, F.U. Abuova, A. Akilbekov, J. Maier, Nucl. Instr. Meth. B 374 (2016) 24.
[37] V.N. Kolobanov, V.V. Mikhailin, S.P. Chernov, D.A. Spassky, V.N. Makhov, M. Kirm, E. Feldbach, S. Vielhauer, J. Phys.: Condensed Matter 21 (2009) 375501.
[38] R.F. Blunt, M.I. Cohen, Phys. Rev. 153 (1967) 1031.
[39] W.A. Sibley, O.E. Faccy, Phys. Rev. 174 (1968) 1076.
[40] O.E. Faccy, W.A. Sibley, Phys. Rev. 186 (1969) 926.
[41] R.T. Williams, C.L. Marquardt, J.W. Williams, M.N. Kabler, Phys. Rev. B 62 (1977) 5003.
[42] A.T. Davidson, J.D. Comins, T.E. Derry, A.M.J. Raphuthi, Phys. Rev. B 48 (1993) 782.
[43] G.O. Amolo, J.D. Comins, A.T. Davidson, A.G. Kozakiewicz, T.E. Derry, D.S. McLachlan, Nucl. Instr. Meth. B 218 (2004) 244.
[44] M.R. Buckton, D. Pooley, J. Phys. C 5 (1972) 1553.
[45] J.L. Kolopus, J.T. Lewis, W.P. Unruh, L.G. Nelson, J. Phys. C: Sol. St. Phys. 4 (1971) 3007.
[46] A.S. El-Said, R. Neumann, K. Schwartz, C. Trautmann, Nucl. Instr. Meth. B 245 (2006) 250.
[47] W.E. Vehse, O.E. Facey, W.A. Sibley, Phys. Status Solidi A 1 (1970) 679.
[48] A.S. El-Said, R. Neumann, K. Schwartz, C. Trautmann, Radiat. Eff. Defects Solids 157 (2002) 649.
[49] M. Nakagawa, M. Okada, K. Atobe, H. Itoh, S. Nakanishi, K. Kondo, Radiat. Eff. Defects Solids 119–121 (1991) 663.
[50] Y. Ueda, J. Phys. Soc. Japan 41 (1976) 1255.
[51] V.N. Kuzovkov, E.A. Kotomin, Rep. Prog. Phys. 51 (1988) 1480.
[52] V.N. Kuzovkov, V.N. Kuzovkov, Rep. Prog. Phys. 55 (1992) 2079.
[53] E.A. Kotomin, V.N. Kuzovkov, Modern aspects of diffusion-controlled reactions. vol. 34 in a series of Comprehensive Chemical Kinetics (Amsterdam: Elsevier, 1996).
[54] V.N. Kuzovkov, E.A. Kotomin, Phys. Status Solidi B 105 (1981) 789.
[55] E.A. Kotomin, V.N. Kuzovkov, Phys. Status Solidi B 108 (1981) 37.
[56] V.N. Kuzovkov, E.A. Kotomin, J. Phys. C: Solid State Phys. 17 (1984) 2284.
[57] V.N. Kuzovkov, E.A. Kotomin, M. Olvera de la Cruz, J. Chem. Phys. 135 (2011) 034702.
[58] V.N. Kuzovkov, G. Zvejnieks, E.A. Kotomin, Phys. Chem. Chem. Phys. 16 (2014) 13974.
[59] V.N. Kuzovkov, E.A. Kotomin, Phys. Chem. Chem. Phys. 16 (2014) 25449.
[60] V.N. Kuzovkov, E.A. Kotomin, A.I.Popov, J. Maier, 2017, in preparation.
[61] E.A. Kotomin, A.I. Popov, Nucl. Instr. Meth. B 141 (1998) 1.
[62] K. Atobe, N. Ishimoto, M. Nakagawa, Phys. Status Solidi A 89 (1985) 155.
[63] M. Izerrouken, T. Benyahia, Nucl. Instr. Meth. B 268 (2010) 2987.